

# A $z = 5.34$ Galaxy Pair in the Hubble Deep Field<sup>1</sup>

Hyron Spinrad, Daniel Stern, Andrew Bunker  
Department of Astronomy, University of California at Berkeley  
Berkeley, CA 94720  
email: (spinrad,dan,bunker)@bigz.Berkeley.edu

Arjun Dey<sup>2</sup>  
Department of Physics & Astronomy, The Johns Hopkins University  
3400 N. Charles St., Baltimore, MD 21218  
email: dey@skysrv.pha.jhu.edu

Kenneth Lanzetta, Amos Yahil, Sebastian Pascarella  
Department of Physics & Astronomy, State University of New York at Stony Brook  
Stony Brook, NY 11794–3800  
email: (lanzetta,ayahil,sam)@sbast3.ess.sunysb.edu

and Alberto Fernández-Soto  
Department of Astrophysics & Optics, University of New South Wales  
Sydney, Australia NSW2052  
email: fsoto@bat.phys.unsw.edu.au

## ABSTRACT

We present spectrograms of the faint  $V$ -drop ( $V_{606} = 28.1, I_{814} = 25.6$ ) galaxy pair HDF 3–951.1 and HDF 3–951.2 obtained at the Keck II Telescope. Fernández-Soto, Lanzetta, & Yahil (1998) derive a photometric redshift of  $z_{\text{ph}} = 5.28_{-0.41}^{+0.34}$  ( $2\sigma$ ) for these galaxies; our integrated spectrograms show a large and abrupt discontinuity near  $7710 \pm 5 \text{ \AA}$ . This break is almost certainly due to the Ly $\alpha$  forest as its amplitude ( $1 - f_{\nu}^{\text{short}}/f_{\nu}^{\text{long}} > 0.87$ , 95% confidence limit) exceeds any discontinuities observed in stellar or galaxian rest-frame optical spectra. The resulting *absorption-break* redshift is  $z = 5.34 \pm 0.01$ .

---

<sup>1</sup>Based on observations at the W.M. Keck Observatory, which is operated as a scientific partnership among the University of California, the California Institute of Technology, and the National Aeronautics and Space Administration. The Observatory was made possible by the generous financial support of the W.M. Keck Foundation.

<sup>2</sup>Hubble Fellow.

Optical/near-IR photometry from the HDF yields an exceptionally red ( $V_{606} - I_{814}$ ) color, consistent with this large break. A more accurate measure of the continuum depression blueward of  $\text{Ly}\alpha$  utilizing the imaging photometry yields  $D_A = 0.88$ .

The system as a whole is slightly brighter than  $L_{1500}^*$  relative to the  $z \sim 3$  Lyman break population and the total star formation rate inferred from the UV continuum is  $\approx 22 h_{50}^{-2} M_{\odot} yr^{-1}$  ( $q_0 = 0.5$ ) assuming the absence of dust extinction. The two individual galaxies are quite small (size scales  $\lesssim 1 h_{50}^{-1}$  kpc). Thus these galaxies superficially resemble the Pascarella et al. (1996) “building blocks”; if they comprise a gravitationally bound system, the pair will likely merge in a time scale  $\sim 100$  Myr.

*Subject headings:* galaxies: distances and redshifts — galaxies: evolution — galaxies : formation — early universe — galaxies: individual: HDF 3–951.0

## 1. Introduction

We are presently targeting photometrically-selected faint galaxies for spectroscopic study at the Keck Telescopes with the goal of measuring redshifts and star-formation rates at early cosmic epochs. Selecting high-redshift galaxies based upon their continuum properties (c.f., Weymann et al. 1998) is important and complements work on emission line-selected galaxies at  $z \gtrsim 4.5$  found serendipitously (Dey et al. 1998) and from narrow-band imaging (Cowie & Hu 1998; Hu, Cowie, & McMahan 1998). Studying galaxies at these high redshifts has important implications for tracing the formation of galaxies and large scale structure, mapping the history of star formation, and understanding the chemical history of the Universe.

The Hubble Deep Field (hereinafter HDF; Williams et al. 1996) has galvanized a renewed effort at estimating photometric redshifts (e.g., Lanzetta, Yahil, & Fernández-Soto 1996; Sawicki, Lin, & Yee 1997; see also Hogg et al. 1998). The extremely deep multiband integrations through the crisp eye of the *Hubble Space Telescope (HST)* supplemented by several deep campaigns across the electromagnetic spectrum (e.g., at radio, sub-millimeter, far-infrared, and near-infrared wavelengths — Fomalont et al. 1997; Hughes et al. 1998; Rowan-Robinson et al. 1997; Hogg et al. 1997; Eisenhardt et al. 1996; Thompson et al. 1998) — are an ideal data set with which to estimate redshifts based upon broad-band colors. High-redshift targets are robustly selected based upon the redshifted Lyman break at  $(1+z) \times 912 \text{ \AA}$  and the redshifted  $\text{Ly}\alpha$  discontinuity at  $(1+z) \times 1216 \text{ \AA}$ , causing the

galaxies to effectively disappear, or “drop out”, at short wavelengths.  $U$ -band dropouts, corresponding to  $z \sim 3$ , have been systematically studied by several groups (c.f., Steidel et al. 1996a; Lowenthal et al. 1997; Spinrad et al. 1998; Bunker et al. 1998).  $B$ -band dropouts, corresponding to  $z \sim 4$ , and  $V$ -band dropouts, corresponding to  $z \sim 5$ , are beginning to be addressed (Dickinson 1998; Weymann et al. 1998; Dey et al. 1998b). Our present list of potential  $z > 4$  candidates ( $B$ - and  $V$ -dropouts) includes six galaxies with  $I_{814} < 26.5$  in the HDF (Fernández-Soto, Lanzetta, & Yahil 1998; AB scale used throughout<sup>3</sup>). Their spectroscopic study, even with the large aperture of the Keck Telescopes and dark sky of Mauna Kea, is clearly a technical challenge. Weymann et al.’s (1998) confirmation of a galaxy at  $z = 5.60$  illustrates that the  $V$ -drop technique works. A systematic survey, however, is necessary to assess that this population is not contaminated by lower-redshift interlopers such as galaxies with extremely high equivalent width emission lines (e.g., [O II] $\lambda$ 3727) in the  $I_{814}$  filter. We describe the observations of one  $V$ -drop system, HDF 3–951.0. Our data imply a redshift of  $z = 5.34$  for this system, one of the highest redshifts yet measured and among the first systematically pre-selected galaxies at  $z > 5$ .

Throughout this paper we adopt  $H_0 = 50 h_{50} \text{ km s}^{-1} \text{ Mpc}^{-1}$ ,  $q_0 = 0.5 (0.1)$ , and  $\Lambda = 0$ . For these parameters,  $1''$  subtends  $5.6 (10.2) h_{50}^{-1} \text{ kpc}$  at  $z = 5.34$  and the Universe is only  $820 \text{ Myr} (1.56 \text{ Gyr})$  old, corresponding to a lookback time of  $93.7\% (90.6\%)$  of the age of the Universe. We present our observations in the following section, our redshift determination in §3, and discuss the galaxy’s inferred properties in §4.

## 2. Observations

HDF 3–951.0 is a faint galaxy “pair”, comprised of HDF 3–951.1 and HDF 3–951.2, near the edge of the WF3 CCD of the HDF. In Fig. 1 we present F606W ( $V_{606}$ ) and F814W ( $I_{814}$ ) images of the galaxy. Extant photometry of this system is assembled in Table 1. Clearly the most outstanding photometric features of the composite (HDF 3–951.0) energy distribution are the non-detection at  $U_{300}$  and  $B_{450}$ , the marginal detection in  $V_{606}$ , and the very red color in  $V_{606} - I_{814}$ . The energy distribution appears to flatten at longer wavelengths with  $I_{814} - K \lesssim 2.0$ . These colors qualitatively suggest a high-redshift, star-forming system with the Ly $\alpha$  forest attenuating the spectrum below  $I_{814}$  and OB stars dominating the rest-frame UV past Ly $\alpha$ . A more detailed technique employing template spectra and

---

<sup>3</sup>The AB magnitude system (Oke 1974) is defined such that  $m_{\text{AB}} = -2.5 \log_{10}(f_{\nu} / \text{erg cm}^{-2} \text{ s}^{-1} \text{ Hz}^{-1}) - 48.60$ .

maximum likelihood analysis yields a photometric redshift of  $z_{\text{ph}} = 5.28_{-0.41}^{+0.34}$  ( $2\sigma$ ) for this system and  $z = 5.72_{-0.34}^{+0.33}$  ( $2\sigma$ ) for HDF 3–951.1 alone (the brighter component; object #3 in Fernández–Soto, Lanzetta, & Yahil 1998; see also Lanzetta, Yahil, & Fernández–Soto 1996). Comparisons between photometric and spectroscopic redshift determinations show that the former is typically robust to  $\Delta z \approx 0.34$  for objects with  $I_{814} \sim 25.5$  and  $z > 3$  (Fernández–Soto, Lanzetta, & Yahil 1998).

However, an accurate determination of the redshift requires deep spectroscopy, and so we observed the HDF during three observing runs in 1998 using the spectroscopic mode of the Low Resolution Imaging Spectrometer (LRIS; Oke et al. 1995) at the Cassegrain focus of the Keck II Telescope. Only the data collected on UT 1998 February 19 were of high quality; UT 1998 January 20 suffered from poor seeing and high cirrus, while integrations on UT 1998 March 28 & 29 were plagued by poor seeing. All observations employed milled slitmasks constructed to allow simultaneous observations of seven  $B$ - and  $V$ -dropout galaxies. The  $1''.5$  wide slitlets were typically  $20''$  long, allowing sufficient slit length for sky subtraction at the expense of a diminished number of targets. Slitmask observations were made at a position angle of  $102.6^\circ$  (east of north) with the 400 l/mm grating ( $\lambda_{\text{blaze}} \approx 8500 \text{ \AA}$ ;  $\Delta\lambda_{\text{FWHM}} \approx 11 \text{ \AA}$ ) sampling the wavelength range  $\lambda\lambda 5940 - 9720 \text{ \AA}$ . Small spatial shifts ( $\approx 4''$ ) were performed between each  $\approx 1800s$  exposure to facilitate removal of fringing in the near-IR regions of the spectrograms.

All data reductions were performed using the IRAF package and followed standard slit spectroscopy procedures. Wavelength calibration was performed using a NeAr lamp, employing telluric lines to adjust the zero-point. Flux calibration was performed using observations of G191B2B, Feige 34, HZ 44, and Wolf 1346 (Massey et al. 1988; Massey & Gronwall 1990) and accurate spectrophotometry was verified against the HDF photometry by convolving the spectra of HDF 3–951.0 and a brighter galaxy which serendipitously lay along one of the slitlets (HDF 3–493.0 —  $I_{814} = 21.74$ ,  $z = 0.848$ ) with the F814W filter response function. HDF 3–951.0 was detected during all three observing runs. However, the February data (seeing  $\sim 0''.7$ , photometric), comprising four integrations totaling 6900s, is of much higher signal-to-noise ratio; our final spectrum (Fig. 2) is composed from the February data alone.

### 3. Redshift Determination

Our final spectrogram of the unresolved pair of faint galaxies (Fig. 2) yields a fairly noisy but robust result: above  $7720 \text{ \AA}$  there is a roughly flat continuum (in  $f_\nu$ ) with a mean flux near  $0.4\mu\text{Jy}$ . Almost no light is detected below  $7700 \text{ \AA}$  ( $f_\nu < 0.05\mu\text{Jy}$ ), and an

accordingly large and abrupt discontinuity exists at  $7710 \pm 5 \text{ \AA}$ . An accurate measurement of the discontinuity wavelength is made difficult by the faint magnitudes considered and the challenges of sky subtraction in the  $7700 \text{ \AA}$  OH sky emission band. We note that the faintness and  $0''.61$  separation of HDF 3–951.1 and HDF 3–951.2 makes separate spectroscopy with ground-based instrumentation exceedingly difficult. Their unusual, yet similar colors, however, support the hypothesis that they lie at the same redshift. Disparate redshifts would lead to a dilution of the  $7710 \text{ \AA}$  break amplitude. The spectrum is also obviously inconsistent with a single high-equivalent width emission line dominating the  $I_{814}$  flux and causing the extremely red  $V_{606} - I_{814}$  color. Our spectrophotometry yields a  $2\sigma$  limit to the equivalent width of an unresolved emission line  $W_{\lambda}^{\text{obs}} < 40 \text{ \AA}$  for  $\lambda > 7800 \text{ \AA}$ . If the red  $V_{606} - I_{814}$  color were due to an extremely strong emission line in  $I_{814}$ , the required equivalent width would be at least  $W_{\lambda}^{\text{obs}} > 200 \text{ \AA}$ , for a constant slope continuum fit to the  $V_{606}$  and  $K$  upper limit magnitudes.

Discontinuities of this amplitude ( $\gtrsim 8$ ) are unprecedented in optical spectra of stars and galaxies. Averaging the spectrum in 10 pixel ( $\approx 18 \text{ \AA}$ ) bins and considering Poissonian counting statistics, we find the average flux density above the discontinuity is  $f_{\nu}^{\text{long}}(\lambda\lambda 8000 - 9000 \text{ \AA}) = 0.432 \pm 0.052 \mu\text{Jy}$ , while the average flux density below the discontinuity is  $f_{\nu}^{\text{short}}(\lambda\lambda 6500 - 7500 \text{ \AA}) = -0.036 \pm 0.038 \mu\text{Jy}$ , i.e., consistent with no observable flux. There is, at this  $\approx 28$  magnitude level, a small systematic problem. The 95% (99%) confidence limit to the amplitude of this continuum depression, calculated from Monte Carlo simulations of the flux densities with the constraint that  $f_{\nu} > 0$ , is then  $1 - f_{\nu}^{\text{short}}/f_{\nu}^{\text{long}} > 0.87$  (0.82). In order of decreasing wavelength, discontinuities are commonly observed in UV/optical spectra of galaxies at rest wavelengths of  $4000 \text{ \AA}$  ( $D(4000)$ ),  $2900 \text{ \AA}$  ( $B(2900)$ ),  $2640 \text{ \AA}$  ( $B(2640)$ ),  $1216 \text{ \AA}$  ( $\text{Ly}\alpha$ ), and  $912 \text{ \AA}$  (the Lyman limit). The hydrogen discontinuities derive from associated and foreground absorption and thus have no theoretical maximum. The longer rest-wavelength discontinuities derive from metal absorption in the stars and galaxies, and are thus dependent upon the age and metallicity of the galaxy (c.f., Fanelli et al. 1992; Spinrad et al. 1997). The largest measured values of  $D(4000)$  in lower-redshift, early-type galaxies are  $\approx 2.6$  (Dressler & Gunn 1990; Hamilton 1985), corresponding to  $1 - f_{\nu}^{\text{short}}/f_{\nu}^{\text{long}} \approx 0.62$ , while *IUE* spectra of main-sequence stars exhibit  $B(2900) \lesssim 3$  and  $B(2640) \lesssim 3$  (Spinrad et al. 1997), corresponding to  $1 - f_{\nu}^{\text{short}}/f_{\nu}^{\text{long}} \lesssim 0.67$ . Therefore, we can safely rule out the low-redshift interpretations of the spectrum of HDF 3–951.0. The  $7710 \text{ \AA}$  break is also unlikely to be associated with a Lyman limit at  $z = 7.45$ ; at that redshift, the  $\text{Ly}\alpha$  forest would likely obliterate the rest-frame  $912 - 1216 \text{ \AA}$  spectrum.  $\text{Ly}\alpha$  itself would be at  $1.03 \mu\text{m}$ , which is a very challenging wavelength for current CCD detectors. Identifying the break with  $\text{Ly}\alpha$  is the lowest redshift and most likely interpretation under these circumstances.

Large breaks are occasionally seen in exotic objects as well. For instance, the iron low-ionization broad absorption line quasar (Fe L $\alpha$ -BAL) FIRST J155633.8+351758 (Becker et al. 1997) has a discontinuity with  $1 - f_{\nu}^{\text{short}}/f_{\nu}^{\text{long}} \approx 0.85$  around 2800 Å. However, this object belongs to an exceedingly rare type of quasar, a classification which we can rule out for HDF 3–951.0 due to its resolved morphology. Furthermore, radio-loud broad absorption line quasars tend to have very red optical/near-IR colors (Hall et al. 1997).

We therefore associate the break with the Ly $\alpha$  forest, implying a redshift  $z = 5.34 \pm 0.01$ . The systematics of Ly $\alpha$  absorption might provide a systematic redward bias of  $\Delta z \approx 0.01$  — in high-redshift galaxies, associated and foreground absorption generally displaces Ly $\alpha$  emission lines redward of their host galaxy systematic velocity by up to several hundred km s $^{-1}$ . In fact, this mechanism also imprints an asymmetry onto the Ly $\alpha$  emission line, when present, thus providing a powerful discriminant between high-redshift Ly $\alpha$  and low-redshift [O II] $\lambda$ 3727 (see Dey et al. 1998a). The sharpness of the discontinuity and the flatness of the longer-wavelength spectrogram (in  $f_{\nu}$ ) are further arguments for identifying the break with the Ly $\alpha$  forest onset. For the remainder of this paper we adopt  $z = 5.34$  for the redshift of the faint galaxy pair HDF 3–951.0.

#### 4. Discussion

Our deep spectroscopy confirming the high-redshift of HDF 3–951.0, as well as Weymann et al. ’s (1998) confirmation of HDF 4–473.0 at  $z = 5.60$ , illustrates that the photometric redshift technique, and, in particular,  $V$ -drop selection, is a robust method for selecting and studying the distant Universe. We now derive some basic physical properties of HDF 3–951.0, consonant with its faint magnitude.

If the UV continuum is dominated by light from young, hot stars, the star-formation rate ( $\dot{M}$ ) may be derived from the UV flux at  $\lambda_0 \gtrsim 1240$  Å. Assuming the continuum emission from HDF 3–951.0 is unreddened and has a spectral slope of  $f_{\nu} \propto \lambda^0$ , consistent with the observations, we derive  $L_{1500} = 22.9 \times 10^{40} h_{50}^{-2} \text{ erg s}^{-1} \text{ \AA}^{-1}$  and  $M_{1500} = -21.5$  AB mag for HDF 3–951.0 based upon the flux density between 8000 and 9000 Å (see Table 1). Madau, Pozzetti, & Dickinson (1998) calculate  $\dot{M} \approx 10^{-40} L_{1500} M_{\odot} \text{ yr}^{-1}$  for  $L_{1500}$  measured in units of  $\text{erg s}^{-1} \text{ \AA}^{-1}$  and a  $> 100$  Myr old population with a Salpeter IMF ( $0.1 < M < 125 M_{\odot}$ ). This is roughly consistent with the relation derived from the Leitherer & Heckman (1995) models for a different IMF and much younger ages of  $< 10$  Myr. These conversions are meant to be illustrative rather than definitive; they depend upon the assumed star-formation history, IMF, metallicity, and age. The lower limit on the inferred star-formation rate for HDF 3–951.0 is thus  $\approx 22 h_{50}^{-2} M_{\odot} \text{ yr}^{-1}$ , assuming

the absence of dust absorption. Dickinson (1998) finds that the ultraviolet luminosity function of Lyman–break galaxies at  $z \approx 3$  is well–modeled by a Schechter luminosity function of characteristic absolute magnitude  $M_{1500}^* \approx -21$  AB mag. This implies that the HDF 3–951.0 galaxies are individually sub–luminous, but slightly brighter than  $L_{1500}^*$  when considered as a single system uncorrected for extinction.

The star–formation rates may also be determined for the galaxy pair individually utilizing the imaging photometry, without reference to the spectrophotometry. Assuming a Heaviside function spectrum with  $f_\nu = 0$  below 7710 Å, and  $f_\nu \propto \lambda^0$  redward of 7710 Å, the  $I_{814}$  magnitudes may be used to calculate an upper limit on the flux density redward of Ly $\alpha$ . This then yields  $F_{1500}$  and, with the above prescription, the inferred star formation rate (see Table 1). We find  $\dot{M} = 13h_{50}^{-2} M_\odot yr^{-1}$  for HDF 3–951.1 and  $\dot{M} = 6h_{50}^{-2} M_\odot yr^{-1}$  for HDF 3–951.2.

The flat red end of the spectrum of HDF 3–951.0 is similar to spectra of  $z \sim 3$  Lyman break galaxies (c.f., Steidel et al. 1996a) — systems which are well–represented by an OB stellar population with little dust. Deep Keck/LRIS spectroscopy of some of the brighter  $z \sim 3$  Lyman break population suggests that galaxies with Ly $\alpha$  in emission are generally flatter in  $f_\nu$  at  $\lambda\lambda 1220 - 1700$  Å, while those galaxies with Ly $\alpha$  in absorption are generally redder at these wavelengths (Spinrad et al. 1998). From a study of vacuum–UV *IUE* spectra of local starburst galaxies, Heckman et al. (1998) find that metal–rich starbursts are redder and more heavily extinguished (have larger values of  $L_{IR}/L_{UV}$ ), have stronger rest–frame UV absorption lines, and occur in more massive and brighter host galaxies. Similarly, the brightest Lyman break galaxies tend *not* to have Ly $\alpha$  in emission (Steidel, private communication), possibly a result of the galaxies lying in deeper potential wells and thus being more able to retain gas and dust which scatter and absorb the Ly $\alpha$  photons and redden the  $\lambda > 1220$  Å continuum. In this scenario, the apparent flatness of our HDF 3–951.0 spectrum at  $\lambda_0 > 1300$  Å is inconsistent with the lack of a measurable Ly $\alpha$  emission line. However, relatively small column densities of neutral gas with even very small dust content can destroy Ly $\alpha$  emission if this gas is static with respect to the ionized region where Ly $\alpha$  photons originate (c.f., Kunth et al. 1998).

HDF 3–951.0 is potentially reddened by foreground and associated dust, consistent with the lack of Ly $\alpha$  emission; our ground–based limits on the near–IR magnitude of the system constrains  $E_{B-V} \lesssim 0.3$  (for a dust–free Heaviside spectrum subject to extinction by a foreground screen of dust following the extinction law of Cardelli, Clayton, & Mathis 1989). This level of extinction would imply intrinsic star formation rates  $\sim 45\%$  higher than the values quoted above. A real measurement of the dustiness of the galaxy pair must await deep near–IR images of the field, as have recently been obtained with NICMOS on

the *HST*.

We next consider the  $I_{814}$  morphology of this system (see Fig. 3). The full-width, half-maxima (FWHM) of HDF 3–951.1 and HDF 3–951.2 are  $0''.50$ , and  $0''.28$  respectively. Comparison with a star reveals that both are clearly resolved ( $\text{FWHM}_{\text{star}} = 0''.14$ ) with deconvolved half-width, half-maxima (HWHM) of  $0''.24$  and  $0''.12$  respectively. For  $q_0 = 0.5$  (0.1), these correspond to 1.3 (2.5)  $h_{50}^{-1}$  kpc for HDF 3–951.1 and 0.7 (1.2)  $h_{50}^{-1}$  kpc for HDF 3–951.2, comparable to the values found for many of the  $z \approx 3$  Lyman-break galaxies (Giavalisco, Steidel, & Macchetto 1996). HDF 3–951.1 (the brighter component) contains sub-structure, with a second “hot spot”  $\sim 0''.12$  east of the core, at a projected separation of 0.66 (1.2)  $h_{50}^{-1}$  kpc. We speculate that this is either a knot of star formation (bright in the rest-frame UV), or evidence of multiple nuclei. The projected proximity of HDF 3–951.2 adds weight to the hypothesis that this is a dynamically-bound system, and that we are witnessing a merger event. Lyman-break galaxies at  $z \approx 3$  often exhibit either disrupted morphologies or multiple components (e.g., Giavalisco, Steidel, & Macchetto 1996; Steidel et al. 1996b; Bunker et al. 1998).

Due to the sub-structure of its core, HDF 3–951.1 is not fit well by either a de Vaucouleurs  $r^{1/4}$  law nor an exponential surface brightness profile. The exponential disk appears to dominate in a two-component model, and the scale length is  $0''.23$ , equivalent to  $r_{\text{disk}} = 1.3$  (2.3)  $h_{50}^{-1}$  kpc. The elongation is  $b/a = 1.2$ .

The fainter HDF 3–951.2 is well-fit by an exponential disk profile, with a scale length of  $0''.12$ , corresponding to 0.65 (1.2)  $h_{50}^{-1}$  kpc, and is almost circular ( $b/a = 1.1$ ). As with the  $z \approx 3$  population, we note that HDF 3–951 is significantly more compact at rest-frame UV wavelengths compared to local disk galaxies, which have typical scale lengths of  $\sim 5$  kpc at optical wavelengths (Freeman 1970).

The angular separation of  $0''.61$  projects to 3.4 (6.2)  $h_{50}^{-1}$  kpc for  $q_0 = 0.5$  (0.1), implying that HDF 3–951.0 is a pair of sub-luminous systems of modest projected separation. What can we say about the evolutionary fate of HDF 3–951.0? Given the small physical sizes and projected separation, in all likelihood HDF 3–951.1 and HDF 3–951.2 will merge into a single galaxy. Assuming a relative velocity of  $\Delta v = 200 \text{ km s}^{-1}$  and a physical separation equal to the projected  $\approx 5$  kpc, the crossing time is  $\approx 25$  Myr. Thus we estimate the merger time scale for HDF 3–951.1 and HDF 3–951.2 is a few crossing times (c.f., Barnes & Hernquist 1996), or  $\sim 100$  Myr. Indeed, we suggest that HDF 3–951.1 and HDF 3–951.2 are already in the process of merging; we are perhaps witnessing the galaxies in a post-collision state, with the luminosity enhanced by merger-induced star formation. Studies of low-redshift merging systems find enhanced rates of star formation (Sanders et al. 1988), consistent with the apparently OB star-dominated spectrum of HDF 3–951.0.



We note that our  $I_{814}$  images sample the rest-frame UV. Even in present-day galaxies, UV-emitting regions in galaxies are typically small. Alternatively, two regions of active star-formation within  $\approx 5$  kpc of each other may well be star-forming knots within the same galaxy. Longer-wavelength imaging will help resolve this question. Indeed, preliminary reductions of NICMOS observations of the HDF suggest that these objects remain separate in F160W images (rest-frame  $\sim 2500$  Å; Dickinson, private communication). We note, finally, that the size and luminosity of HDF 3–951.0 suggest it to be a more distant version of the  $z \approx 2.4$  galaxies discussed by Pascarelle et al. (1996) which have typical half-light radii of  $0''.1 - 0''.2$ .

What are the implications of the large continuum discontinuities in the Ly $\alpha$  region? How reliable is the nominal factor of 10 at 95% confidence level we suggest, and how does it propagate to the  $D_A$  parameter (Oke & Korycansky 1982, Madau 1995, Schneider et al. 1991ab)? The largest discontinuities previously measured in quasar spectra at  $z \gtrsim 4.5$  are approximately a factor of 4 (see Fig. 4). Our determination of the  $f_\nu$  break amplitude for HDF 3–951.0 is made difficult since the composite galaxy spectrum is very faint at  $\lambda\lambda 6500 - 7700$  Å. Oke & Korycansky (1982) define  $D_A$  as

$$D_A \equiv \left\langle 1 - \frac{f_\nu(\lambda\lambda 1050 - 1170)_{\text{obs}}}{f_\nu(\lambda\lambda 1050 - 1170)_{\text{pred}}} \right\rangle.$$

From the February 1998 data, we measure average flux densities of  $f_\nu(\lambda\lambda 1050 - 1170) = -0.029 \pm 0.045 \mu\text{Jy}$  and  $f_\nu(\lambda\lambda 1250 - 1370) = 0.405 \pm 0.055 \mu\text{Jy}$ . The implied 95% (99%) confidence limit to  $D_A$  is then  $D_A > 0.82$  (0.75). The 1998 January and March data qualitatively support our large amplitude break, but quantitatively do not aid our numerical evaluation of it. Larger values are possible and future, more sensitive observations will determine a more precise value of  $D_A$  for this system.

Alternatively, we can produce a photometric estimate of  $D_A$  utilizing the Williams et al. (1996) broad band colors, the *HST*/WFPC2 filter curves, and the plausible assumption (born out by our spectra to date) that the  $f_\nu$  flux distributions above and below Ly $\alpha$  are flat. We assume a two-step spectral energy distribution with zero flux below the Lyman limit,  $f_\nu^-$  between the Lyman limit and Ly $\alpha$ , and  $f_\nu^+$  redwards of Ly $\alpha$ . For  $f_\nu^\pm \propto \lambda^0$ , 54% of the F606W flux comes from  $\lambda > 5782$  Å (the Lyman limit at  $z = 5.34$ ) and 48% of the F814W flux comes from  $\lambda > 7710$  Å (Ly $\alpha$  at  $z = 5.34$ ). For the observed magnitudes of HDF 3–951.0, this implies  $f_\nu^- = 0.04 \mu\text{Jy}$  and  $f_\nu^+ = 0.33 \mu\text{Jy}$ . The resultant “photometric Ly $\alpha$ discontinuity”, with  $V - I = 2.50$  is  $D_A^{\text{phot}} = 0.88$ . This agrees with the break amplitude derived from the Keck spectrogram and is much higher than previously reported values of  $D_A$  (also see Dey et al. 1998). In Fig. 4 we present recent measurements of  $D_A$  from spectra of quasars and high-redshift galaxies, where HDF 3–951.0 is indicated by the more robust

photometric measurement. The Weymann et al. (1998) points utilize their photometry, corrected for the Ly $\alpha$  emission line flux of  $1.0 \times 10^{-17}$  erg cm $^{-2}$  s $^{-1}$ , and a  $f_\nu \propto \lambda^\beta$  spectrum fit to the NICMOS near-IR brightnesses (top point). The lower Weymann et al. (1998) point utilizes an  $f_\nu \propto \lambda^{-0.4}$  spectrum, corresponding to their best-fit semi-empirical model.

Our concern about the break amplitude arises from its strength: Madau’s (1995) theoretical estimate of the contribution of the Ly $\alpha$  forest to  $D_A$  is only  $\approx 0.79$  at  $z = 5.34$  and  $\approx 0.83$  at  $z = 5.60$ . This extrapolation assumes a distribution of high and low optical depth foreground Ly $\alpha$  clouds causing Lyman series absorption in the spectrum of a distant quasar or galaxy. The scatter around the Madau curve is substantial, even at lower redshifts, so the high values of  $D_A$  at  $z > 5$  may simply reflect the usual scatter observed in that parameter. However, at large enough redshift our line of sight *must* penetrate the end stages of reionization (c.f., Loeb 1998; Miralda-Escudé & Rees 1997) where a smooth distribution of neutral hydrogen gas will cause an additional Gunn-Peterson H I opacity at  $\lambda < 1216$  Å. Whether this starts at  $z = 5$  or  $z \gtrsim 10$  remains an intriguing question. Are we seeing the first hints of the Gunn-Peterson trough in these distant systems? If we see enhanced (Gunn-Peterson) absorption short-ward of Ly $\alpha$  (corresponding to  $z \sim 5$ ) relative to the expected thickening of the Ly $\alpha$  forest, one might begin to further exploit spectrophotometry of these distant galaxies in a novel and useful manner.

We thank J. Aycock, W. Wack, R. Quick, T. Stickel, G. Punawai, R. Goodrich, R. Campbell, T. Bida, and B. Schaeffer for their invaluable assistance during our observing runs at the W.M. Keck Observatory. We are grateful to A. Philips for providing software and assistance in slitmask construction and alignment and J. Cohen for supporting LRIS; and to M. Dickinson, E. Gawiser, J.R. Graham, C. Manning, F. Marleau, and C. Steidel for useful comments. We also thank the referee, D.W. Hogg, for timely and constructive comments. H.S. acknowledges support from NSF grant AST 95-28536, D.S. acknowledges support from IGPP grant 99-AP026, A.B. acknowledges support from a NICMOS postdoctoral fellowship, A.D. acknowledges support from NASA grant HF-01089.01-97A, K.L. acknowledges support from NASA grant NAGW-4422 and NSF grant AST-9624216, A.F.-S. acknowledges support from an Australian ARC grant.

## REFERENCES

- Barnes, J.E. & Hernquist, L. 1996, ApJ, 471, 115  
 Becker, R.H., Gregg, M.D., Hook, I.M., McMahon, R.G., White, R.L., & Helfand, D.J. 1997, ApJ, 479, L93

- Bunker, A. et al. 1998, in preparation
- Cardelli, J.A., Clayton, G.C., & Mathis, J.S. 1989, *ApJ*, 345, 245
- Cowie, L.L. & Hu, E.M. 1998, *AJ*, 115, 1319
- Dey, A., Spinrad, H., Stern, D., Graham, J.R., & Chaffee, F. 1998a, *ApJ*, 498, L93
- Dey, A., et al. 1998b, in preparation
- Dickinson, M.E. 1998, in Proc. STScI 1997 May Symp., *The Hubble Deep Field*, ed. M. Livio, S.M. Fall, & P. Madau (Cambridge: Cambridge Univ. Press), in press
- Dressler, A. & Gunn, J.E. 1990, in Proc. Hubble Centennial Symp., ASP vol. 10, 200
- Eisenhardt, P., Dickinson, M., Stanford, S.A., Elston, R., & Bershadsky, M. 1996, *BAAS*, #103.06
- Fanelli, M.N., O’Connell, R.W., Burstein, D., & Wu, C.C. 1992, *ApJS*, 82, 197
- Fernández-Soto, A., Lanzetta, K., & Yahil, A. 1998, *ApJ*, in press
- Fomalont, E., Kellerman, K., Richards, E., Windhorst, R., & Partridge, R. 1997, *ApJ*, 496, 93
- Franx, M., Illingworth, G., Kelson, D., van Dokkum, P., & Tran, K. 1997, *ApJ*, 486, L75
- Freeman, K.C. 1970, *ApJ*, 160, 811
- Giavalisco, M., Steidel, C., & Macchetto, D. 1996, *ApJ*, 470, 189
- Hall, P., Martini, P., DePoy, D.L., & Gatley, I. 1997, *ApJ*, 484, L17
- Hamilton, D. 1985, *ApJ*, 297, 371
- Heckman, T.M., Robert, C., Leitherer, C., Garnett, D., & van der Rydt, F. 1998, astro-ph/9803185
- Henry, J., et al. 1994, *AJ*, 107, 1270
- Hogg, D.W., Neugebauer, G., Armus, L., Matthews, K., Pahre, M., Sofier, B.T., & Weinberger, A.J. 1997, *AJ*, 113, 2338
- Hogg, D.W., et al. 1998, *AJ*, 115, 1418
- Hu, E.M., Cowie, L.L., & McMahon, 1998, *ApJ*, 502, 99
- Hughes, D. et al. 1998, *Nature*, 394, 241
- Kennefick, J., Djorgovski, S.G., & de Carvalho, R. 1995 *AJ*, 110, 2553
- Kunth, D., Mas-Hesse, J.M., Terlevich, E., Terlevich, R., Lequeux, J., & Fall, S.M. 1998, *A&A*, 334, 11
- Leitherer, C. & Heckman, T. 1995, *ApJS*, 96, 9

- Lanzetta, K., Yahil, A., & Fernández–Soto, A. 1996, *Nature*, 381, 759
- Loeb, A. 1998, in *Proc. Science with the Next Generation Space Telescope*, ASP Conf. Ser. 133, ed. E.P. Smith & A. Koratkar, 73
- Lowenthal, J. et al. 1997, *ApJ*, 481, 673
- Madau, P. 1995, *ApJ*, 441, 18
- Madau, P., Pozzetti, L., & Dickinson, M. 1998, *ApJ*, 498, 106
- Massey, P., Strobel, K., Barnes, J.V., & Anderson, E. 1988, *ApJ*, 328, 315
- Massey, P. & Gronwall, C. 1990, *ApJ*, 358, 344
- Miralda–Escudé, J. & Rees, M.J. 1997, *ApJ*, 478, L57
- Oke, J.B. 1974, *ApJS*, 27, 21
- Oke, J.B. et al. 1995, *PASP*, 107, 375
- Oke, J.B. & Korycansky, D.G. 1982, *ApJ*, 225, 110
- Pascarelle, S.M., Windhorst, R.A., Keel, W.C., & Odewahn, S.C. 1996, *Nature*, 383, 45
- Rowan–Robinson, M. et al. 1997, *MNRAS*, 289, 490
- Sanders, D. et al. 1988, *ApJ*, 325, 74
- Sawicki, M.J., Lin, H., & Yee, H.K.C. 1997, *AJ*, 113, 1
- Schneider, D., Schmidt, M., & Gunn, J. 1989, *AJ*, 98, 1507
- Schneider, D., Schmidt, M., & Gunn, J. 1991a, *AJ*, 101, 2004
- Schneider, D., Schmidt, M., & Gunn, J. 1991b, *AJ*, 102, 837
- Smith, J., Djorgovski, S., Thompson, D., Brisken, W., Neugebauer, G., Matthews, K., Meylan, G., Piotto, G., & Suntzeff, N. 1994, *AJ*, 108, 1147
- Spinrad, H., Dey, A., Stern, D., Dunlop, J., Peacock, J., Jimenez, R., & Windhorst, R. 1997, *ApJ*, 484, 581
- Spinrad, H., Dey, A., Stern, D., & Bunker, A. 1998, in *Proc. Know Colloq.*, ed. H. Röttgering, in press
- Steidel, C.C., Giavalisco, M., Pettini, M., Dickinson, M., & Adelberger, K. 1996a, *ApJ*, 462, L17
- Steidel, C.C., Giavalisco, M., Dickinson, M., & Adelberger, K. 1996b, *AJ*, 112, 352
- Thompson, R. et al. 1998, in preparation
- Weymann, R., Stern, D., Bunker, A., Spinrad, H., Chaffee, F., Thompson, R., & Storrie–Lombardi, L. 1998, *ApJ*, in press

Williams, R. et al. 1996, AJ, 112, 1335

Zuo, L. & Lu, L. 1993, ApJ, 418, 601

Table 1. Photometry.

| Galaxy Component       | $V_{606}$ | $I_{814}$ | $K$    | $\langle F_{1500} \rangle$ <sup>§</sup> | $L_{1500} h_{50}^2$ <sup>†</sup> | $\dot{M} h_{50}^2$ <sup>‡</sup> |
|------------------------|-----------|-----------|--------|---|----------------------------------|---------------------------------|
| HDF 3–951.1 (brighter) | 28.68     | 26.20     | ...    | 8.0                                     | 12.7                             | 13                              |
| HDF 3–951.2 (fainter)  | 28.87     | 26.95     | ...    | 4.0                                     | 6.3                              | 6                               |
| HDF 3–951.0 (sum)      | 28.08     | 25.60     | > 23.6 | 13.9 (14.4) <sup>††</sup>               | 22.1 (22.9) <sup>††</sup>        | 22 (23) <sup>††</sup>           |

Note. — All magnitudes are in the AB system. Separation of component centers is 0".61. Optical isophotal magnitudes are from Williams et al. (1996),  $2\sigma$  limit on the near-IR magnitude is derived from ground-based observations with IRIM (Eisenhardt et al. 1996) for a bidimensional Gaussian with FWHM  $\approx 1".20$ . HDF 3–951 is undetected in  $U_{300}$  and  $B_{450}$ , implying  $2\sigma$  limiting magnitudes of  $U_{300} > 28.2$  and  $B_{450} > 28.9$ . The small inconsistency in that  $I_{\text{HDF 3–951.0}} < I_{\text{HDF 3–951.1}} + I_{\text{HDF 3–951.2}}$  is present in Williams et al. (1996) and likely derives from the faint magnitudes and close separations considered.

<sup>§</sup>Flux density at 1500 Å,  $F_{1500}$ , is in units of  $10^{-20} \text{ erg s}^{-1} \text{ cm}^{-2} \text{ Å}^{-1}$  and is derived from  $I_{814}$  assuming a  $f_{\nu} \propto \lambda^0$  spectrum for  $\lambda > 7710 \text{ Å}$  with no flux below 7710 Å. See text for details.

<sup>††</sup>First value derives from photometry, second (parenthetical) value derives from spectrophotometry utilizing the continuum flux near 1350 Å and assuming a  $f_{\nu} \propto \lambda^0$  spectrum. See text for details.

<sup>†</sup> $L_{1500}$  is in units of  $10^{40} \text{ erg s}^{-1} \text{ Å}^{-1}$ , calculated for  $q_0 = 0.5$  using  $F_{1500}$  values.

<sup>‡</sup>Star-formation rates, in units of  $M_{\odot} \text{ yr}^{-1}$ , assume  $q_0 = 0.5$  and a Salpeter IMF with  $0.1 < M < 125 M_{\odot}$  (see Madau, Pozzetti, & Dickinson 1998 for details). For  $q_0 = 0.1$  these rates are  $\approx 3.3$  times larger.

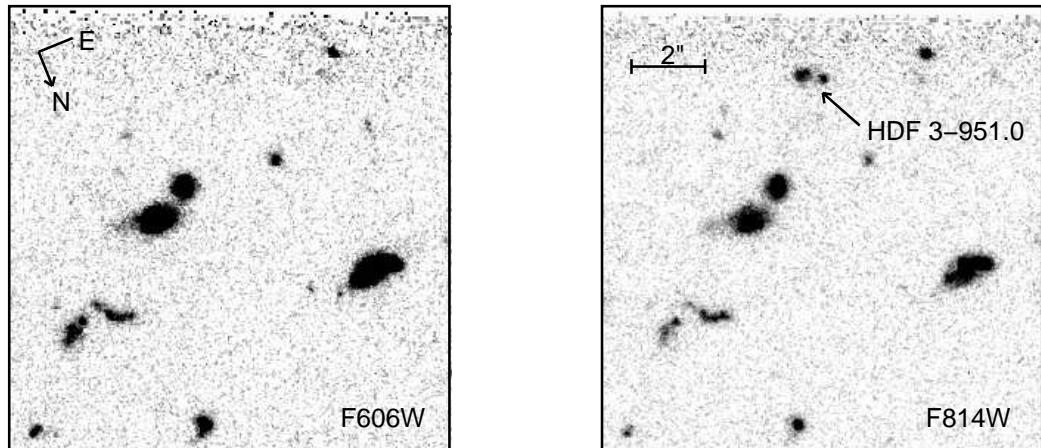


Fig. 1.— *HST* F606W (left) and F814W (right) drizzled images of HDF 3-951.0, a  $z = 5.34$  galaxy pair comprised of HDF 3-951.1 (SW, brighter) and HDF 3-951.2 (NE, fainter). HDF 3-951.0 is located at

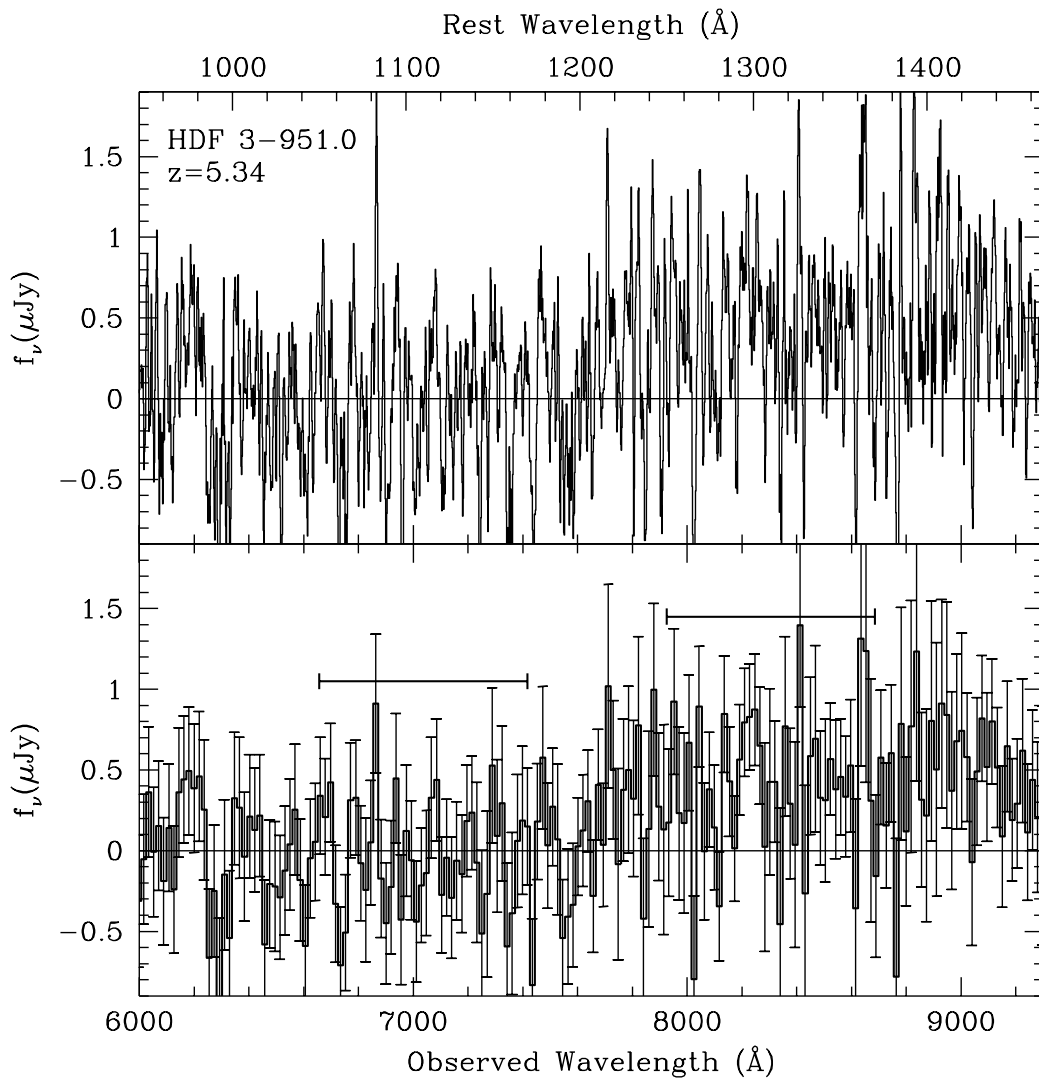


Fig. 2.— Spectrum of the color-selected galaxy HDF 3-951.0 at  $z = 5.34$ . Top spectrum is smoothed with a 5 pixel boxcar filter, bottom spectrum is co-averaged in 10 pixel bins with  $1\sigma$  error bars assigned according to sky counts. The total exposure time is 6900s, and the spectrum was extracted using an  $1''.3 \times 1''.5$  aperture. Horizontal bars on the bottom panel indicates the wavelength region considered for determination of  $D_A$ .



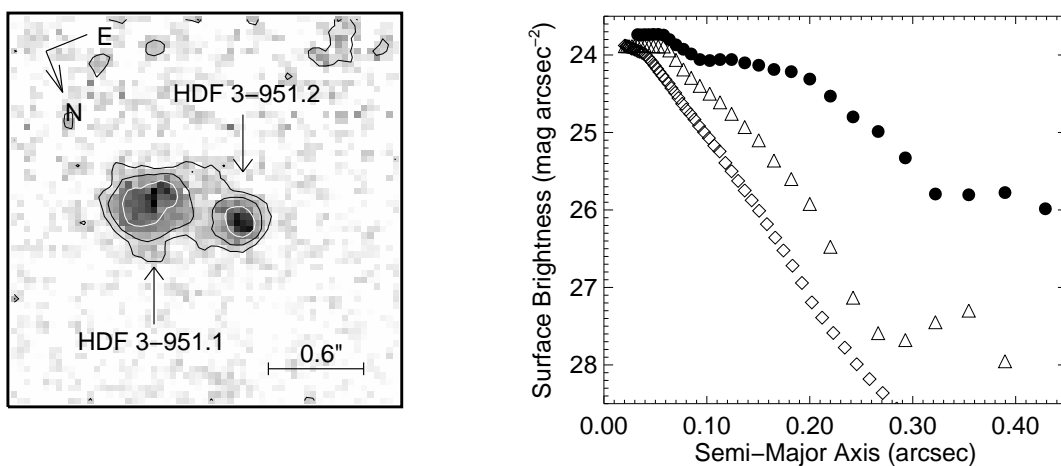


Fig. 3.— Detail of the drizzled F814W ( $I_{814}$ ) image of HDF 3-951.0 (left) and surface brightness profiles for the individual components (right). The scaled surface brightness profile of a star is illustrated (open diamonds); both components of HDF 3-951.0 are clearly resolved. Note that the brighter component (HDF 3-951.1; solid circles) has a sub-structure to the east, possibly indicative of a recent or ongoing interaction. The surface brightness profile clearly illustrates this sub-structure. The fainter component (HDF 3-951.2; open triangles) is well-fit by an exponential disk profile. The flatness of the surface brightness profiles at small ( $\lesssim 0''.05$ ) radii are due to sampling the same pixel, and at large radii ( $\gtrsim 0''.3$ ), the profiles of the galaxies are contaminated by their respective neighbors.

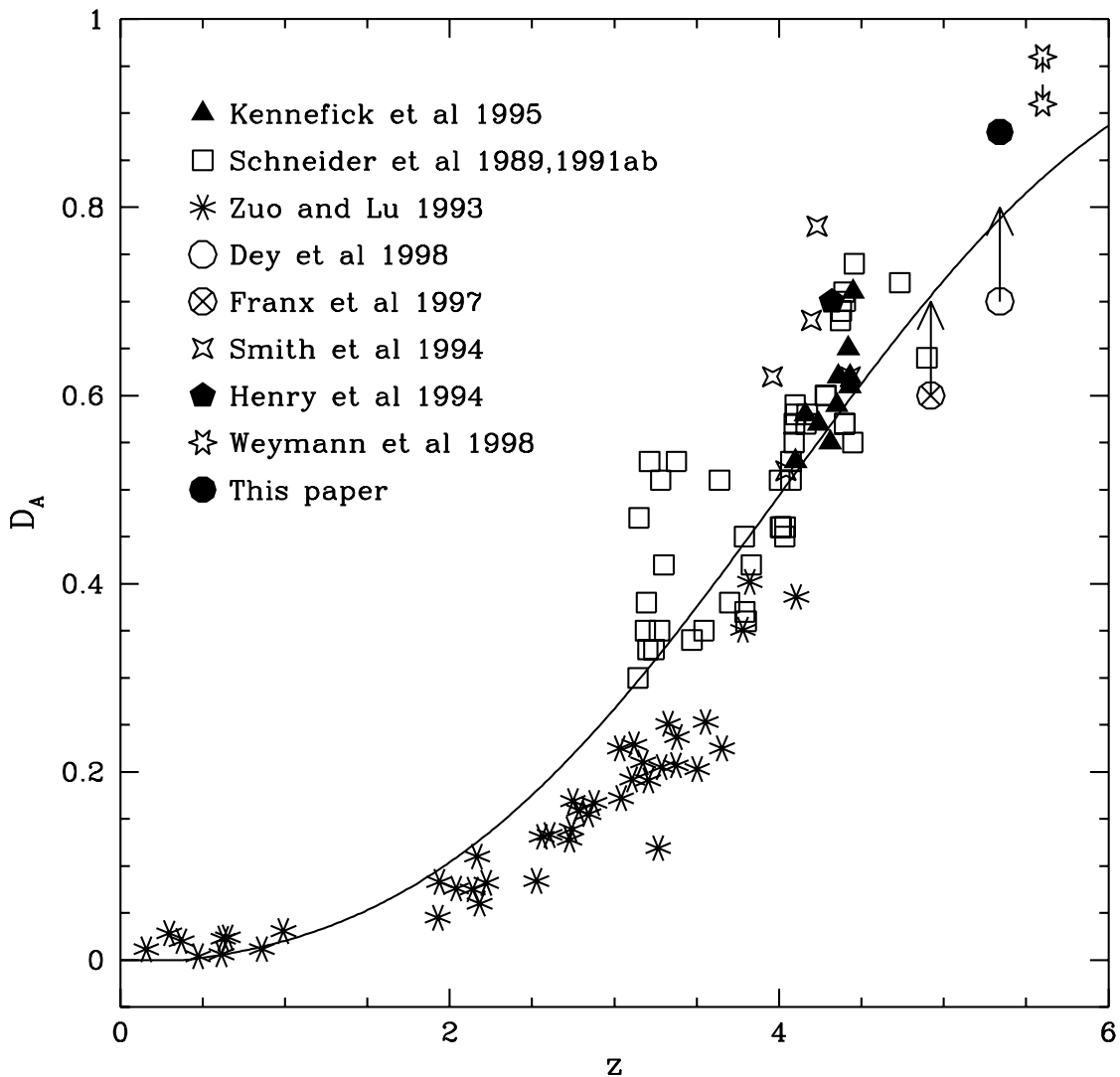


Fig. 4.— Values of the continuum depression blueward of  $\text{Ly}\alpha$  ( $D_A$ ) plotted as a function of redshift, with the Madau (1995) model overplotted as a solid line. See text for details regarding derivation of  $D_A$  for HDF 3–951.0 (this paper; photometric measurement) and HDF 4–473.0 (Weymann et al. 1998). The apparent systematic displacement of the Zuo & Lu (1994) points likely derives from their revised approach for determining the continuum blueward of  $\text{Ly}\alpha$ : employing high signal-to-noise, high resolution spectra, they model and replace the  $\text{Ly}\alpha$  forest absorption features.